Synthesis, Characterization, and Properties of High Molecular Weight Unsymmetrically Substituted Poly(ferrocenylsilanes)

Daniel Foucher, Ralf Ziembinski, Ruth Petersen, John Pudelski, Mark Edwards, Yizeng Ni, Jason Massey, C. Raimund Jaeger, G. Julius Vancso,* and Ian Manners*

Department of Chemistry, University of Toronto, 80 St. George Street, Toronto M5S 1A1, Ontario, Canada

Received March 1, 1994; Revised Manuscript Received April 21, 1994®

ABSTRACT: A series of high molecular weight, unsymmetrically substituted poly(ferrocenylsilanes) [Fe-(η-C_5H_4)$_2$(SiRR′)]$_n$ (**4a–4g**) (**a** R = Me, R′ = H; **b** R = Me, R′ = $CH_2CH_2CF_3$; **c** R = Me, R′ = CH=CH_2; **d** R = Me, R′ = n-$C_{18}H_{37}$; **e** R = Me, R′ = Ph; **f** R = Me, R′ = Fc, Fc = (η-C_5H_4)Fe(η-C_5H_5); **g** R = Me, R′ = Nor, Nor = 5-norbornyl) have been prepared via the thermal ring-opening polymerization of the corresponding strained, silicon-bridged [1]ferrocenophanes Fe(η-C_5H_4)$_2$(SiRR′) (**3a–3g**). The latter species were prepared via the reaction of Fe(η-C_5H_4Li)$_2$·tmeda (tmeda = tetramethylethylenediamine) with the appropriate unsymmetrical dichloroorganosilane RR′$SiCl_2$. The poly(ferrocenylsilanes) **4a–4g** were structurally characterized by ^{1}H, ^{13}C, and ^{29}Si NMR spectroscopy and by elemental analysis. The molecular weights of polymers **4a–4g** were estimated to be in the range $\bar{M}_w = 1.6 \times 10^5$–$2.7 \times 10^6$ and $\bar{M}_n = 7.1 \times 10^4$–$8.1 \times 10^5$ by GPC using polystyrene standards. In addition, the solution behavior of a moderate molecular weight sample of **4e** was investigated by low-angle laser light scattering, which yielded an absolute value of $\bar{M}_w = 8.54 \times 10^4$ and a second virial coefficient $A_2 = 3.3 \times 10^{-4}$ mol cm^2 g^{-2} in THF at 20 °C. The thermal transition behavior of polymers **4a–4g** was investigated by DSC. Glass transition temperatures were found to vary with the substituents at silicon and were in the range of 1 °C (for **4d**) to 99 °C (for **4f**). A strong melting endotherm for **4d** at 16 °C was detected by both DSC and DMA and annealed samples of **4a** showed very weak melt endotherms at 87 and 102 °C. None of the other polymers showed evidence for melting transitions. WAXS analysis confirmed that **4b–4g** are essentially amorphous at 25 °C whereas **4a** is more ordered. The electrochemical behavior of **4a–4g** was investigated by cyclic voltammetry, and **4a–4e** and **4g** showed two oxidation waves, which is consistent with the presence of significant interactions between the iron centers. The cyclic voltammogram of **4f** was more complex and indicated that interactions exist between the iron centers in the polymer backbone and the ferrocenyl side groups.

Introduction

The development and study of new polymer systems which contain transition metals in the main chain is an area of intense current interest as a result of their potentially attractive and useful physical and chemical properties.[1,2] Nevertheless, synthetic routes to well-defined, high molecular weight and soluble examples of these materials remain limited. In 1992 we reported the discovery of the ring-opening polymerization (ROP) of strained, silicon-bridged [1]ferrocenophanes **1** which

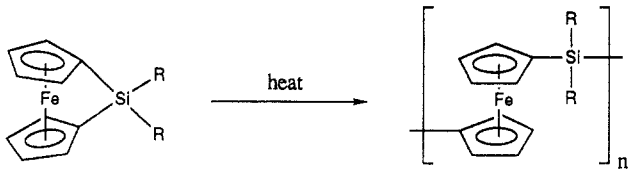

1 **2**

R = Me, Et, n-Bu, or n-Hex

provided access to the first examples of high molecular weight poly(ferrocenylsilanes) **2**.[3] This ROP route has subsequently been extended to a variety of [1]ferrocenophanes, including those which contain other inorganic elements in the bridge structure, and also to [2]-metallocenophanes.[4–8] Studies of the properties of symmetrically substituted poly(ferrocenylsilanes) **2** have shown that these interesting materials function as pyrolytic precursors to iron silicon carbide ceramics, possess unusual electrochemical characteristics which indicate that the iron atoms interact with one another, and in some cases form ordered structures in the solid state.[3,6–11] As part of our efforts to further understand the characteristics of poly(ferrocenylsilanes) we report in this paper our work on the synthesis, characterization, and properties of a series of unsymmetrically substituted poly(ferrocenylsilanes) prepared via this novel ROP route.[12,13]

Experimental Section

Materials. Solvents were dried by standard methods, distilled, and stored under nitrogen over activated molecular sieves. Dichlorosilanes were purchased from Hüls USA and were distilled before use. Tetramethylethylenediamine (TMEDA) and trichloromethylsilane were purchased from Aldrich and were distilled before use. Ferrocene and 1.6 M butyllithium in hexanes were also purchased from Aldrich and were used as received. Dilithioferrocene·tmeda[14a] and (chloromercurio)ferrocene[14b] were prepared according to literature procedures.

Equipment. ^{1}H NMR spectra (200 or 400 MHz), ^{13}C NMR spectra (50.3 or 100.5 MHz), ^{29}Si NMR spectra (79.8 MHz), and ^{19}F NMR spectra (282.3 MHz) were recorded on either Varian Gemini 200 or 300 instruments or a Varian Unity 400 spectrometer. NMR chemical shifts were referenced to residual protonated solvent peaks. Mass spectra were obtained with the use of a VG 70–250S mass spectrometer operating in electron impact (EI) mode. Molecular weights were estimated by gel permeation chromatography (GPC) using a Waters Associates liquid chromatograph equipped with a 510 HPLC pump, U6K injector, Ultrastyragel columns with a pore size between 10^3 and 10^5 Å, and a Waters 410 differential refractometer. A flow rate of 1.0 mL/min was used, and samples were dissolved in a solution of 0.1% tetra-n-butylammonium bromide in THF. Ten samples of monodisperse polystyrene in the range $M_w = 10^3$–10^6 were used as standards for calibration purposes. Elemental analyses were

® Abstract published in *Advance ACS Abstracts*, June 1, 1994.

0024-9297/94/2227-3992$04.50/0

performed by the Canadian Microanalytical Service Ltd., Delta, BC, Canada.

Static light scattering experiments on polymer **4e** were carried out by the low-angle laser light scattering (LALLS) technique, utilizing a Chromatix KMX-6 instrument at a wavelength of 632.8 nm and a scattering angle of 6–7°. Measurements were carried out at room temperature (20 °C) using a metal cell 4.93 mm in length. Each solution was filtered a minimum of three times through a Sartorius regenerated cellulose membrane filter with a 0.45-μm average pore size and once through a 0.2-μm disposable filter before injection into the sample cell. The value of the refractive index increment dn/dc (0.2139 ± 0.0005 mL/g) of the polymer solutions was obtained by using a Chromatix KMX-16 differential refractometer operating at a wavelength of 632.8 nm. The instrument was calibrated with NaCl solutions. Prior to LALLS measurements the UV–vis spectrum of the polymer was checked for possible absorption at the wavelength used in the light scattering experiment. Characteristic absorptions of the polymer were well removed from the working wavelength.

A Perkin-Elmer DSC-7 differential scanning calorimeter equipped with a TAC 7 instrument controller was used to study polymer thermal behavior. Thermograms were calibrated with the melting transitions of decane and indium and were obtained at a heating rate of 10 °C/min under dinitrogen. A Perkin-Elmer DMA 7 instrument operated by a PE 7700 computer was utilized to study the mechanical performance of selected samples. The temperature dependence of the E-modulus and of the phase angle δ was measured by applying an oscillating uniaxial compressive force on a gumlike sample of polymer **4d**. The temperature was varied from −60 to +50 °C with a heating rate of 10 °C/min.

Electrochemical experiments were carried out using a PAR Model 273 potentiostat with a Pt working electrode, a W secondary electrode, and an Ag wire reference electrode in a Luggin capillary. Polymer solutions were 5×10^{-3} M in CH_2Cl_2 with 0.1 M $[Bu_4N][PF_6]$ as a supporting electrolyte. Peak currents were found to be proportional to the square root of the scan rate over the range studied (25 to 1000 mV s^{-1}), which indicates that charge transfer is similar to a semiinfinite linear diffusion process.

Wide angle X-ray scattering data were obtained using a Siemens D5000 diffractomer employing Ni filtered Cu Kα (λ = 1.541 78 Å) radiation. The samples were scanned at step widths of 0.02° with 1.0 s per step in the Bragg angle range 3–40°. Samples for the X-ray studies were prepared by spreading the finely ground polymer on grooved glass slides.

Synthesis of Ferrocenylmethyldichlorosilane, FcMeSiCl$_2$. This compound has been previously reported,[15] but full synthetic details were not published. A 1.6 M hexanes solution of n-BuLi (13.1 mL, 21 mmol) was added dropwise via syringe to a cool (0 °C) solution of (chloromercurio)ferrocene[14b] (4.00 g, 9.5 mmol) in ether (50 mL). The resulting mixture was maintained at this temperature for 1 h and was then stirred at room temperature for 1 h. The mixture was then cooled to −78 °C and treated with $MeSiCl_3$ (1.2 mL, 10 mmol) via syringe. The mixture was then allowed to warm to 25 °C, and after stirring overnight, the resulting dark red solution was filtered and the filtrate was concentrated in vacuo. The crude material was purified via distillation under reduced pressure. After removal of the $Hg(n\text{-}Bu)_2$ byproduct (bp 50 °C, 1 mmHg), the desired dichlorosilane was collected as a red liquid (bp 130 °C, 0.05 mmHg). Upon cooling, 0.60 g (23%) of $FcSiMeCl_2$ was obtained as a dark red crystalline solid: ^{29}Si NMR (C_6D_6) δ 22.4 ppm; ^{13}C NMR (C_6D_6) δ 73.4 (Cp), 72.7 (Cp), 69.7 (η-C_5H_5), 66.9 (Cp C–Si), −6.2 (CH_3) ppm; ^{1}H NMR (C_6D_6) δ 4.09 (s, 4 H, η-C_5H_4), 3.96 (s, 5 H, η-C_5H_5), 0.68 (s, 3 H, CH_3) ppm; MS (EI, 70 eV) m/z (%) 298 (100, M$^+$), 263 (15, M$^+$ − Cl), 233 (28, M$^+$ − Cp).

Synthesis of the Unsymmetrically Substituted Silicon-Bridged [1]Ferrocenophanes 3a–3g. Ferrocenophanes **3a** and **3g** were prepared from reaction of $Fe(\eta\text{-}C_5H_4Li)_2$·tmeda with the appropriate dichloroorganosilane by our modification[8a,b] of the methods reported initially by Osborne and then by Wrighton.[16] Ferrocenophanes **3a–3c**, **3e**, and **3f** were purified by high vacuum sublimation (130–150 °C, 5×10^{-3} mmHg), and the yields were 80% for **3a**, 42% for **3b**, 60% for **3c**, 40% for **3e**, and 21% for **3f**, respectively. Ferrocenophane **3d** was purified by high vacuum distillation (160 °C, 5×10^{-3} mmHg) to give a red-orange semisolid in 30% yield. Ferrocenophane **3g** was purified by recrystallization from hexanes and was obtained in 50% yield.

For **3a**: red-orange crystals; ^{29}Si NMR ($CDCl_3$) δ −21.2 ($^1J_{SiH}$ = 210 Hz) ppm; ^{13}C NMR (C_6D_6) δ 78.1 (Cp), 77.7 (Cp), 76.4 (Cp), 75.0 (Cp), 27.7 (Cp C–Si), −5.7 (CH_3) ppm; ^{1}H NMR (C_6D_6) δ 5.43 (q, $^3J_{HH}$ = 3.6 Hz, 1 H, Si–H), 4.41–4.38 (m, 4 H, Cp), 4.18 (m, 2 H, Cp), 3.96 (m, 2 H, Cp), 0.44 (d, $^3J_{HH}$ = 3.6 Hz, 3 H, CH_3) ppm; MS (EI, 70 eV) m/z (%) 228 (100, M$^+$), 213 (72, M$^+$ − CH_3), 157 (13, M$^+$ − CH_3 − Fe).

For **3b**: red-orange crystals; ^{29}Si NMR (C_6D_6) δ −2.8 ppm; ^{19}F NMR (C_6D_6) δ −68.4 (t, $^3J_{FH}$ = 10.4 Hz) ppm; ^{13}C NMR (C_6D_6) δ 128.3 (q, J_{CF} = 275 Hz, $CH_2CH_2CF_3$), 78.1 (Cp), 77.9 (Cp), 75.6 (Cp), 75.4 (Cp), 31.1 (Cp C–Si), 27.5 (q, J_{CF} = 30 Hz, $CH_2CH_2CF_3$), 5.1 (q, J_{CF} = 1.7 Hz, $CH_2CH_2CF_3$), −5.8 (Si–CH_3) ppm; ^{1}H NMR (C_6D_6) δ 4.35 (m, 4 H, Cp), 3.84 (m, 2 H, Cp), 3.74 (m, 2 H, Cp), 1.98 (m, 2 H, $SiCH_2CH_2CF_3$), 1.00 (m, 2 H, $SiCH_2CH_2CF_3$), 0.16 (s, 3 H, CH_3) ppm; MS (EI, 70 eV) m/z (%) 324 (100, M$^+$), 247 (28, M$^+$ − Me − $CH_2CH{=}CF_2$), 227 (16, M$^+$ − $CH_2CH_2CF_3$).

For **3c**: red crystals; ^{29}Si NMR (C_6D_6) δ −12.4 ppm; ^{13}C NMR (C_6D_6) δ 135.0 (−CH=CH_2), 134.7 (−CH=CH_2), 77.88 (Cp), 77.84 (Cp), 76.0 (Cp), 75.6 (Cp), 31.9 (Cp C–Si), −4.1 (CH_3) ppm; ^{1}H NMR (C_6D_6) δ 6.33 (dd, $^3J_{HH}$ = 14.3 Hz, 14.3 Hz, 1 H, −CH=CH_2), 6.13 (dd, $^3J_{HH}$ = 14.3, 3.9 Hz, 1 H, −CH=$CH_{trans}H_{cis}$), 6.08 (dd, $^3J_{HH}$ = 14.3, 3.9 Hz, 1 H, −CH=$CH_{trans}H_{cis}$), 4.40 (m, 4 H, Cp), 4.09 (m, 2 H, Cp), 3.95 (m, 2 H, Cp), 0.44 (s, 3 H, CH_3) ppm; MS (EI, 70 eV) m/z (%) 254 (100, M$^+$), 239 (36, M$^+$ − CH_3), 213 (100, M$^+$ − CH_3 − C_2H_2).

For **3d**: red-orange semisolid; ^{29}Si NMR (C_6D_6) δ −3.1 ppm; ^{13}C NMR (C_6D_6) δ 77.7 (Cp), 77.6 (Cp), 75.9 (Cp), 75.7 (Cp), 33.9 ($C_{16}H_{32}CH_2CH_3$), 32.4 (Cp C–Si), 30.3 (12 interior–CH_2), 30.2 ($C_{15}H_{30}CH_2CH_2CH_3$), 23.3 ($SiCH_2CH_2CH_2C_{15}H_{32}$), 23.2 ($SiCH_2CH_2C_{16}H_{34}$), 14.4 ($C_{17}H_{34}CH_3$), 13.3 ($SiCH_2C_{17}H_{36}$), −4.9 (Si–$CH_3$) ppm; ^{1}H NMR ($C_6D_6$) δ 4.47 (m, 4 H, Cp), 4.03 (m, 2 H, Cp), 3.98 (m, 2 H, Cp), 0.86–1.80 (m, 37 H, $C_{18}H_{37}$), 0.42 (s, 3 H, Si–CH_3) ppm; MS (EI, 70 eV) m/z (%) 480 (100, M$^+$), 409 (7, M$^+$ − CH_3 − Fe), 227 (37, M$^+$ − $C_{18}H_{37}$).

For **3e**: red-orange crystals; ^{29}Si NMR (C_6D_6) δ −10.9 ppm; ^{13}C NMR (C_6D_6) δ 136.5 (ipso-Ph), 133.9 (*o*-Ph), 130.4 (*p*-Ph), 128.2 (*m*-Ph), 78.1 (Cp), 77.9 (Cp), 76.7 (Cp), 76.0 (Cp) 32.2 (Cp C–Si), 1.7 (CH_3) ppm; ^{1}H NMR (C_6H_6) δ 7.89 (br s, 2 H, Ph), 7.24 (br m, 3 H, Ph), 4.13–3.96 (m, 8 H, Cp), 0.53 (s, 3 H, CH_3) ppm; MS (EI, 70 eV) m/z (%) 304 (40, M$^+$), 289 (10, M$^+$ − CH_3), 234 (100, M$^+$ − CH_2 −Fe).

For **3f**: red-orange powder; ^{29}Si NMR (C_6D_6) δ −10.4 ppm; ^{13}C NMR (C_6D_6) δ 77.9 (Cp), 77.6 (Cp), 76.2 (Cp), 75.6 (Cp), 74.2 (Cp), 71.7 (Cp), 70.6 (Fc, C_{ipso}–Si), 68.9 (η-C_5H_5), 28.8 (Cp C_{ipso}–Si), −4.1 (CH_3) ppm; ^{1}H NMR (C_6D_6) δ 4.44 (m, $^3J_{HH}$ = 1.6 Hz, 2 H, Cp), 4.26–4.03 (m, 15 H, Cp, and Fc), 0.62 (s, 3 H, CH_3) ppm; MS (EI, 70 eV) m/z (%) 412 (100, M$^+$), 347 (28, M$^+$ − C_5H_5), 227 (13, M$^+$ − Fc).

For **3g**: red-orange powder; ^{29}Si NMR (C_6D_6) δ −1.7 (s, endo 33%), −2.6 (s, exo 66%) ppm; ^{13}C NMR (C_6D_6) δ 138.3 (−CH=CH, endo), 136.2 (−CH=CH, exo), 134.8 (−CH=CH, exo), 134.1 (−CH=CH, endo), 77.7–77.6 (Cp, endo and exo), 76.1–75.9 (Cp, endo and exo), 51.5 (bridge −CH_2, exo), 47.9 (bridge −CH_2, endo), 44.7 (exo), 43.1 (endo), 42.9 (exo), 42.8 (endo), 33.6 (Cp C–Si, exo), 33.1 (Cp C–Si, endo), 27.5 (−CH_2, exo), 26.9 (−CH_2, endo), 22.9 (exo), 22.8 (endo), −4.9 (s, CH_3, exo), −5.8 (s, CH_3, endo) ppm; ^{1}H NMR (C_6D_6) *endo isomer* (33%) δ 6.19 (q, $^3J_{H_eH_d}$ = 5.5 Hz, $^3J_{H_eH_f}$ = 3.0 Hz, H_e), 5.98 (q, ^3J = 5.7, 3.0 Hz, 1 H, H_f), 4.45 (m, 4 H, Cp), 3.99 (m, 2 H, Cp), 3.93 (m, 2 H, Cp), 3.18–3.10 (br m, 2 H, H_i, H_h), 2.0–1.0 (s, 5 H, H_a, H_b, H_c, H_d, H_g), 0.33 (s, 3 H, CH_3); ^{1}H NMR (C_6D_6) *exo isomer* (66%) δ 6.13 (q, $^3J_{H_eH_d}$ = 5.6, $^3J_{H_eH_f}$ = 2.9 Hz, H_e), 5.94 (q, ^3J = 5.7, 2.9 Hz, 1 H, H_f), 4.42 (m, 4 H, Cp), 4.08 (m, 2 H, Cp), 3.95 (m, 2 H, Cp), 2.88–2.83 (m, 2 H, H_i, H_h), 2.0–1.0 (s, 5 H, H_a, H_b, H_c, H_d, H_g), 0.26 (s, 3 H, CH_3) ppm; MS (EI, 70 eV) m/z (%) 320 (52, M$^+$), 254 (100, M$^+$ − CpH), 213 (22, M$^+$ − CH_3 − C_2H_2 − C_5H_6).

The ratio of *endo*-**3g** and *exo*-**3g** isomers was determined by ^{1}H NMR integration. The resonances were assigned by comparison to other ferrocenylnorbornyl derivatives.[17]

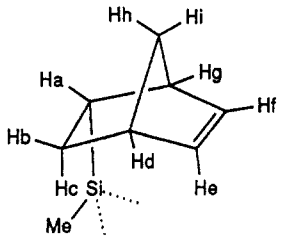

endo-3g (33%)

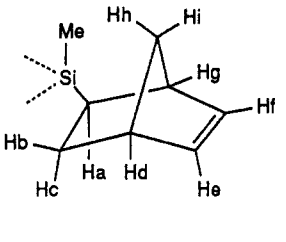

exo-3g (66%)

ROP of 3a–3g: Synthesis of the Unsymmetrically Substituted Poly(ferrocenylsilanes) 4a–4g. Polymers **4a–4g** were prepared similarly, and the general synthesis is illustrated by that of **4a**. A sample of **3a** (1.00 g, 4.39 mmol) was heated in an evacuated, sealed Pyrex tube at 130 °C for 1 h. After the initial melt, an increase in viscosity was immediately observed, and after 10 min, the tube contents were immobile. The polymeric product was dissolved in THF (40 mL) over 4 h, and the resulting solution was concentrated to 10 mL. The polymer solution was then added dropwise to stirred hexanes (300 mL) and the precipitated polymer was collected by filtration, redissolved in THF (30 mL), and reprecipitated into methanol (500 mL). The yellow, fibrous product was then dried in vacuo to afford 0.90 g (90%) of **4a**. The yields of purified **4b–4g** were in the range 80–95%. In the case of polymer **4d**, the THF polymer solution was precipitated twice into methanol.

For **4a**: yellow powder; ^{29}Si NMR ($CDCl_3$) δ −20.0 ($^1J_{SiH}$ = 51 Hz) ppm; ^{13}C NMR ($CDCl_3$) δ 74.8 (Cp), 74.2 (Cp), 72.3 (Cp), 72.2 (Cp), 72.2 (Cp C–Si), −4.4 (CH_3) ppm; ^{1}H NMR (C_6D_6) δ 5.24 (br s, 1 H, Si–H), 4.30 (br s, 4 H, Cp), 4.25 (s, 2 H, Cp), 4.16 (s, 2 H, Cp), 0.61 (s, 3 H, CH_3) ppm. Anal. Calcd for $C_{11}H_{12}FeSi$: C, 57.9; H, 5.3. Found: C, 53.7; H, 5.1. GPC: M_w = 8.6 × 10^5, M_n = 4.2 × 10^5, polydispersity (M_w/M_n) = 2.0.

For **4b**: yellow fibrous powder; ^{29}Si NMR (C_6D_6) δ −4.3 ppm; ^{19}F NMR (C_6D_6) δ −68.2 (br s) ppm; ^{13}C NMR (C_6D_6) δ 130 (q, J_{CF} = 275 Hz, $CH_2CH_2CF_3$), 73.8 (Cp), 73.6 (Cp), 72.2 (Cp), 72.0 (Cp), 69.4 (Cp C–Si), 35.2 (m, $CH_2CH_2CF_3$), 8.63 (br s, $CH_2CH_2CF_3$), −1.8 (Si–CH_3) ppm; ^{1}H NMR (C_6D_6) δ 4.25 (br s, 4 H, Cp), 3.96 (br s, 4 H, Cp), 2.01 (2 H, $SiCH_2CH_2CF_3$), 1.25 (br s, 2 H, $SiCH_2CH_2CF_3$), 0.43 (s, 3 H, CH_3) ppm. Anal. Calcd for $C_{14}H_{15}F_3FeSi$: C, 51.9; H, 4.6. Found: C, 50.2; H, 4.9. GPC: M_w = 2.7 × 10^6, M_n = 8.1 × 10^5, polydispersity (M_w/M_n) = 3.4.

For **4c**: yellow powder; ^{29}Si NMR (C_6D_6) δ −12.9 ppm; ^{13}C NMR (C_6D_6) δ 138.4 (−CH=CH_2), 132.7 (−CH=CH_2), 74.0 (2 C, Cp), 72.0 (Cp), 71.5 (Cp), 69.7 (Cp C–Si), −2.8 (CH_3) ppm; ^{1}H NMR (C_6D_6) δ 6.4–5.8 (br s, 3 H, CH=CH_2), 4.5–3.8 (br m, 8 H, Cp), 0.35 (br s, 3 H, CH_3) ppm. Anal. Calcd for $C_{13}H_{14}FeSi$: C, 61.4; H, 5.5. Found: C, 60.9; H, 6.2. GPC: M_w = 1.6 × 10^5, M_n = 7.7 × 10^4, polydispersity (M_w/M_n) = 2.1.

For **4d**: dark orange elastomer; ^{29}Si NMR (C_6D_6) δ −5.3 ppm; ^{13}C NMR (C_6D_6) δ 71.9 (Cp), 70.8 (Cp), 69.4 (Cp), (Cp C–Si, not located), 32.2 ($C_{16}H_{32}CH_2CH_3$), 31.2 ($C_{15}H_{30}CH_2CH_2CH_3$), 30.0 (12 interior −CH_2), 24.8 ($SiCH_2CH_2CH_2C_{15}H_{32}$), 23.2 ($SiCH_2CH_2C_{16}H_{34}$), 17.0 ($SiCH_2C_{17}H_{35}$), 14.5 ($C_{17}H_{34}CH_3$), −1.5 (Si–$CH_3$) ppm; ^{1}H NMR ($C_6D_6$) δ 4.2 (br s, 8H, Cp), 1.80–0.86 (br s, 37 H, $C_{18}H_{37}$), 0.60 (s, 3 H, CH_3) ppm. Anal. Calcd for $C_{29}H_{48}SiFe$: C, 72.5; H, 10.1. Found: C, 70.1; H, 9.5. GPC: (sample 1) peak 1 M_w = 1.4 × 10^6, M_n = 5.6 × 10^5, polydispersity (M_w/M_n) = 2.5; peak 2 M_w = 3.4 × 10^3, M_n = 3.0 × 10^3, polydispersity (M_w/M_n) = 1.1. GPC: (sample 2) M_w = 2.6 × 10^4, M_n = 1.65 × 10^4, polydispersity (M_w/M_n) = 1.6.

For **4e**: red-orange powder; ^{29}Si NMR (C_6D_6) δ −10.9 ppm; ^{13}C NMR (C_6D_6) δ 138.3 (ipso-Ph), 134.7 (*o*-Ph), 129.3 (*p*-Ph), 128.0 (*m*-Ph), 74.5 (Cp), 74.2 (Cp), 72.4 (Cp), 72.0 (Cp), 70.3 (Cp C–Si), −2.4 (CH_3) ppm; ^{1}H NMR (C_6D_6) δ 7.90 (m, 2 H, *o*-Ph), 7.25 (m, 3 H, *m*- and *p*-Ph), 4.13–4.07 (m, 8H, Cp), 0.75 (s, 3H, CH_3) ppm. Anal. Calcd for $C_{17}H_{16}FeSi$: C, 67.1; H, 5.3. Found: C, 66.7; H, 5.4. GPC: (sample 1) M_w = 3.0 × 10^5, M_n = 1.5 × 10^5, polydispersity (M_w/M_n) = 2.0; (sample 2) (used for LALLS) M_w = 5.8 × 10^4, M_n = 3.4 × 10^4.

For **4f**: yellow powder; ^{29}Si NMR (C_6D_6) δ −9.8 ppm; ^{13}C NMR (C_6D_6) δ 74.3 (Cp), 74.0 (Cp), 72.1 (Cp), 71.85 (Fc, C_{ipso}–Si), 71.82 (Cp C_{ipso}–Si), 71.2 (Cp), 69.0 (η-C_5H_5), −5.6 (CH_3) ppm; ^{1}H NMR (C_6D_6) δ 4.0–4.4 (m, 17 H, Cp), 0.87 (s, 3 H, CH_3) ppm. Anal. Calcd for $C_{21}H_{20}SiFe_2$: C, 61.2; H, 4.9. Found: C, 57.2; H, 4.8. GPC: M_w = 1.6 × 10^5, M_n = 7.1 × 10^4, polydispersity (M_w/M_n) = 2.2.

For **4g**: bright yellow powder; ^{29}Si NMR (C_6D_6) δ −3.4 (br s, endo and exo) ppm; ^{13}C NMR (C_6D_6) δ 138.8 (−CH=CH, endo), 135.6 (−CH=CH, exo), 134.6 (−CH=CH, exo), 134.3 (−CH=CH, endo), 74.5 (Cp, endo and exo), 72.1 (Cp, Cp_{ipso} endo and exo), 51.9 (bridge −CH_2, exo), 47.2 (bridge −CH_2, endo), 46.1 (exo), 44.4 (endo), 43.1 (endo and exo), 29.0 (−CH_2, endo and exo), 25.6 (endo and exo), −2.6 (CH_3, exo), −3.1 (CH_3, endo) ppm; ^{1}H NMR (C_6D_6) δ 6.35 (br s, endo andexo H_e), 6.04 (br m, endo and exo H_f), 4.30 (br s, 4 H, endo and exo Cp), 4.17 (br s, 4 H, endo and exo Cp), 3.55–2.86 (m, 2 H, endo and exo H_c, H_d), 2.0–1.0 (br m, 5 H, endo and exo H_a, H_b, H_g, H_i, H_j), 0.62 (br s, 3 H CH_3, exo), 0.45 (br s, 3 H CH_3, endo) ppm. Anal. Calcd for $C_{18}H_{20}FeSi$: C, 67.5; H, 6.3. Found: C, 65.7; H, 6.2. GPC: M_w = 1.6 × 10^5, M_n = 1.1 × 10^4, polydispersity (M_w/M_n) = 1.5.

Light Scattering Measurements for 4e in THF. Static light scattering experiments in the low-angle regime were used to determine the weight average molar mass $\bar{M}_w$ and the second virial coefficient A_2 of a sample of **4e**. The values of $\bar{M}_w$ were obtained from the Rayleigh–Debye relationship, in the limit of low scattering angles, θ, as previously described.[8a]

Results and Discussion

Silicon-bridged [1]ferrocenophanes **1** have been known since 1975.[16a] These molecules have been shown to possess strained structures in which the planes of the cyclopentadienyl ligands are tilted relative to one another, usually by ca. 21°.[8b,16] We recently reported that these species undergo thermally induced ROP when heated at elevated temperatures to yield high molecular weight poly(ferrocenylsilanes) **2**.[3] Most of the subsequently published work concerning these macromolecules has involved polymers which are symmetrically substituted at silicon.[6–11] In this paper we describe details of the synthesis, characterization, and studies of the thermal transition behavior and electrochemistry of a series of unsymmetrically substituted poly(ferrocenylsilanes).

Synthesis and Structural Characterization of the Unsymmetrically Substituted Silicon-Bridged [1]-Ferrocenophanes 3a–3g. The unsymmetrically substituted silicon-bridged [1]ferrocenophanes, **3a–3g**, with alkyl and aryl groups at silicon were prepared via salt elimination reactions of Fe(η-C_5H_4Li)$_2$·tmeda (tmeda = tetramethylethylenediamine) with the appropriate organochlorosilane RR′$SiCl_2$. This method is similar to that used previously to prepare symmetrically substituted analogues.[3,8a] The new ferrocenophanes **3a–3c**, **3e**, and **3f** were purified by high vacuum sublimation, while **3d** was purified by high vacuum distillation to yield a semisolid. Ferrocenophane **3g** was recrystallized from hexanes and was obtained as a red-orange powder. In all cases, the monomers were moisture sensitive and samples of these species were therefore stored and manipulated under an inert dinitrogen atmosphere.

Ferrocenophanes **3a–3g** were characterized by ^{29}Si, ^{1}H, and ^{13}C NMR spectroscopy and by mass spectrometry. The ^{29}Si NMR chemical shifts for **3b**, **3d**, and **3g** (−1.7 to −3.1 ppm) were similar to those previously found for the symmetrically substituted silicon-bridged [1]ferrocenophanes **1** (R = Me, Et, *n*-Bu, or *n*-Hex) (−1.4 to −4.6 ppm).[8a] By contrast, a ^{29}Si NMR resonance at −21.2 ppm was found for **3a** which possesses an Si–H bond. A large one bond Si–H coupling ($^1J_{SiH}$ = 210 Hz) was detected for this species, which is typical of other silanes containing an Si–H bond.[18] By comparison, the presence of sp^2 hybridized carbon atoms at silicon as in **3c**, **3e**, and **3f** led to ^{29}Si NMR resonances with chemical shifts closer to that found

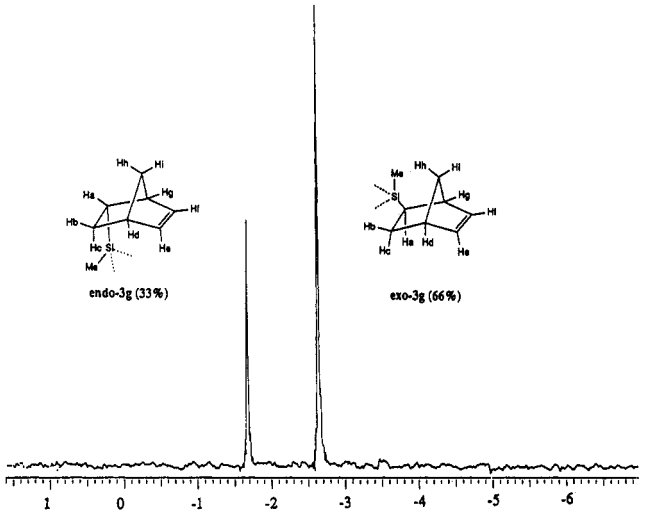

Figure 1. ^{29}Si NMR (79.8 MHz, C_6D_6) spectrum of **3g** showing the presence of both endo and exo isomers.

for the phenylated species **1** (R = Ph) at −11.7 ppm. The ^1H and ^{13}C spectra of ferrocenophanes **3a–3g** were generally more complex than those of the symmetrical ferrocenophanes **1**,[8a] as the point group symmetry is lowered to C_s from C_{2v}. Thus, for example, the ^{13}C NMR spectra of **3a–3g** showed the presence of five unique carbon atoms in the cyclopentadienyl region rather than the three detected for the symmetrically substituted analogues **1** (R = Me, Et, *n*-Bu, and *n*-Hex).[8a] The chemical shifts of the ipso carbon atoms present in these species, like those of the symmetrical species **1**, are located ca. 40 ppm upfield from the ipso shifts observed for unbridged ferrocenylsilanes.[8a,16d] A $^{13}C/^1H$ NMR heteronuclear correlation experiment for **3a** showed that the order of shielding of the ^1H and ^{13}C resonances was identical. The peak pattern for the proton resonances in the cyclopentadienyl region for all the unsymmetrical species **3a–3g** was essentially identical with two, usually overlapping, multiplets at 4.4–4.5 ppm and two well separated multiplets at 3.9 and 4.1 ppm, respectively. The norbornyl methyl derivative **3g** was obtained as a 1:2 mixture of endo and exo isomers, as determined by ^{29}Si NMR (see Figure 1) and ^1H NMR spectroscopy. The ^1H and ^{13}C chemical shifts of the norbornyl group were assigned on the basis of previously known derivatives,[17] in conjuction with an APT sequence experiment for the ^{13}C NMR resonances which identified the bridgehead atoms. The mass spectra of **3a–3g** were consistent with the assigned structures and showed peaks arising from the molecular ions and logical fragmentation products.

ROP of 3a–3g: Synthesis and Structural Characterization of the Poly(ferrocenylsilanes) 4a–4g. ROP of the unsymmetrical ferrocenophane monomers **3a–3c** and **3e–3f** was achieved by heating these species in the melt at elevated temperatures in evacuated, sealed Pyrex tubes, as reported previously for their symmetrical substituted analogues **1** (Scheme 1).[3,8a] In all cases the tube contents became molten, then rapidly more viscous, and eventually immobile. The poly(ferrocenylsilane) **4d** was isolated from the thermal distillation of **3d**, in a manner similar to the preparation of **2** (R = *n*-Hex) from **1** (R = *n*-Hex), as reported previously.[8a]

The polymeric products **4a–4g** dissolved slowly, but completely in THF which indicated that no appreciable cross-linking had taken place at this stage. The polymers were then purified by precipitation into hexanes or methanol. The highly soluble polymer **4b** could be readily solution cast into thin translucent films from solvents such as toluene or THF. Brittle films of polymers **4a**, **4c**, and **4e–4g** were similarly prepared. Polymer **4d** was isolated at room temperature as a dark orange gum which was readily soluble in nonpolar organic solvents such as hexanes. While polymers **4a–4g** appeared to be stable to the atmosphere, samples of **4a** and **4c** which had been exposed to moisture or left in the air for prolonged periods were found to be virtually insoluble in organic solvents after precipitation and drying. These polymers did swell appreciably, suggesting that cross-linking had occurred. It is possible that the Si–H groups present in **4a** slowly hydrolyze to form Si–O–Si linkages between the polymer chains, whereas cross-linking of **4c** through the vinyl groups is also possible.

Scheme 1

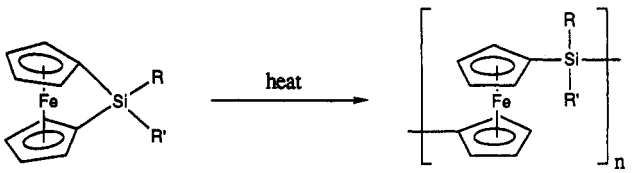

3 **4**

- **a** R = Me, R' = H
- **b** R = Me, R' = $CH_2CH_2CF_3$
- **c** R = Me, R' = $CH{=}CH_2$
- **d** R = Me, R' = *n*-$C_{18}H_{37}$
- **e** R = Me, R' = Ph
- **f** R = Me, R' = Fc (Fc = $(\eta\text{-}C_5H_4)Fe(\eta\text{-}C_5H_5)$)
- **g** R = Me, R' = Nor (Nor = 5-norbornyl)

Table 1. Molecular Weight, ^{29}Si NMR, and Thermal Transition Data for the Unsymmetrical Poly(ferrocenylsilanes) 4a–4g

polymer	R	R'	$\bar{M}_w$[a]	$\bar{M}_n$[a]	$\delta(^{29}Si)$ (ppm)[b]	T_g (°C)
4a	Me	H	8.6×10^5	4.2×10^5	−20.0	9[c]
4b	Me	$CH_2CH_2CF_3$	2.7×10^6	8.1×10^5	−4.3	59
4c	Me	$CH{=}CH_2$	1.6×10^5	7.7×10^4	−12.9	28
4d	Me	*n*-$C_{18}H_{37}$	1.4×10^6	5.6×10^5[d]	−5.3	1[e]
4e	Me	Ph	3.0×10^5	1.5×10^5	−10.9	54
4f	Me	Fc[f]	1.6×10^5	7.1×10^4	−9.8	99
4g	Me	Nor[f]	1.6×10^5	1.1×10^5	−3.4	81

[a] Estimated by GPC in THF using polystyrene standards. [b] ^{29}Si spectra were recorded in C_6D_6 except for that of **4a** which was recorded in $CDCl_3$. [c] Melting endotherms at 87 and 102 °C were detected for the annealed polymer. [d] A bimodal molecular weight distribution was found for this polymer sample. Molecular weights of $\bar{M}_w = 3.4 \times 10^3$ and $\bar{M}_n = 3.0 \times 10^3$ were observed for the oligomeric fraction. [e] A melting endotherm at 16 °C was detected for this polymer. [f] Fc = ferrocenyl $[(\eta\text{-}C_5H_4)Fe(\eta\text{-}C_5H_5)]$, Nor = 5-norbornyl.

Poly(ferrocenylsilanes) **4a–4g** were structurally characterized in solution by ^{29}Si, ^{13}C, and ^1H NMR spectroscopy and were also characterized by elemental analysis. In addition, estimates of the molecular weight of the polymers were obtained by gel permeation chromatography (GPC) and in one case by low-angle laser light scattering (LALLS).

The ^{29}Si NMR data and GPC data for **4a–4g** are summarized in Table 1. The ^{29}Si NMR signals of the unsymmetrically substituted poly(ferrocenylsilanes) **4b–4d** and **4g** were found 1–3 ppm upfield relative to those of their corresponding strained silicon-bridged [1]ferrocenophane precursors. A similar shift inthe ^{29}Si NMR resonances relative to the corresponding monomers was previously observed for symmetrically substituted poly-

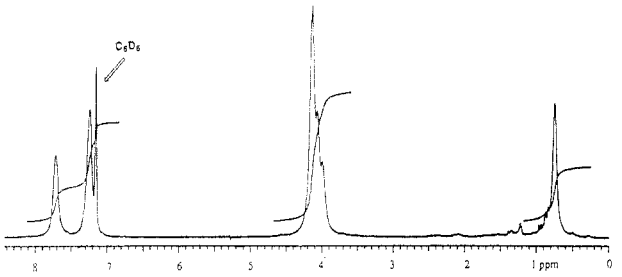

Figure 2. ^{1}H NMR spectrum (200 MHz, C_6D_6) of poly(ferrocenylsilane) **4e**.

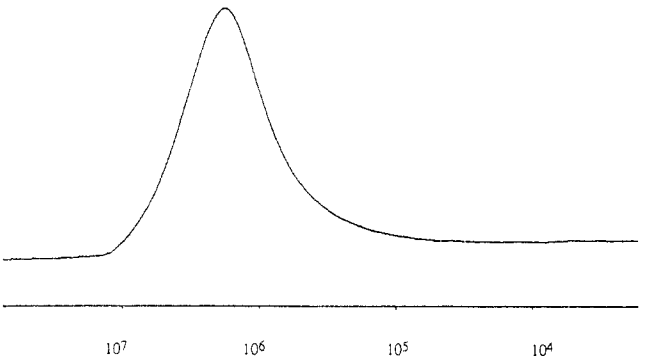

Figure 3. GPC trace of poly(ferrocenylsilane) **4b** in THF using polystyrene standards for column calibration.

(ferrocenylsilanes) **2**.[8a] In the case of polymers **4a** and **4f**, ^{29}Si NMR resonances at −20.0 and −9.8 ppm were detected, respectively. These are slightly downfield from those of the ferrocenophanes **3a** (−21.2 ppm) and **3f** (−10.4 ppm). The ^{29}Si NMR spectrum of the methyl norbornyl polymer **4g** consisted of a single, broad resonance centered at −3.4 ppm whereas that of the monomer **3g** showed singlet resonances at −1.7 and −2.6 ppm for the exo and endo isomers present. Broad, less well-resolved resonances were found in the ^{13}C NMR spectra of the unsymmetrically substituted poly(ferrocenylsilanes) **4a–4g** compared to those of the symmetrical analogues **2**. This might be attributed to the conformational complexity of the unsymmetrical polymers arising from the presence of syndiotactic, isotactic, or atactic configurations. However, these microstructures could not be distinguished by NMR for any of the poly(ferrocenylsilanes) studied. The ^{13}C NMR ipso carbon resonances of polymers **4a–4g** showed a downfield shift to more conventional values of ca. 70–72 ppm compared to those of the monomers **3a–3g** (ca. 28–32 ppm), as was found previously for the symmetrical poly(ferrocenylsilanes) **2**. The ^{1}H NMR spectra of **4a–4g** (in C_6D_6) showed the expected integration ratios among the number of protons present in their different chemical environments. This is illustrated for the case of **4e** in Figure 2.

GPC analysis of the polymers **4a–4g** revealed that high molecular weight material ($\bar{M}_w$ = 1.6 × 10^5–2.7 × 10^6, $\bar{M}_n$ = 7.1 × 10^4–8.1 × 10^5) was obtained in all cases, even when the side groups were sterically demanding ferrocenyl or norbornyl substituents (Table 1). A representative chromatogram is shown for **4b** in Figure 3. The molecular weights obtained were found to be noticeably dependent on the monomer purity. For instance, in the case of polymer **4f**, sublimation of monomer **3f** once followed by ROP afforded material of moderately high molecular weight ($\bar{M}_w$ = 4.5 × 10^4, $\bar{M}_n$ = 2.6 × 10^4) whereas polymerization of a twice-sublimed sample of **3f** afforded material with a molecular weight that was significantly higher ($\bar{M}_w$ = 1.6 × 10^5, $\bar{M}_n$ = 7.1 × 10^4). A bimodal molecular weight distribution was found for polymer **4d**, with both high molecular weight and essentially oligomeric fractions (see Table 1). Subsequent, carefully controlled polymerization reactions of **3d** have afforded monomodal **4d** of moderately high molecular weight ($\bar{M}_w$ = 2.6 × 10^4, $\bar{M}_n$ = 1.65 × 10^4).

In order to investigate the solution properties of an unsymmetrical poly(ferrocenylsilane) and to provide an absolute determination of the molecular weight, LALLS studies were performed on THF solutions of a moderate molecular weight sample of polymer **4e**, which was selected as a representative example. An absolute $\bar{M}_w$ for the polymer **4e** of (8.54 ± 0.04) × 10^4 was obtained from the LALLS study. There is a significant experimental difference (31%) between the absolute $\bar{M}_w$ obtained from LALLS for this sample and that obtained from GPC measurements ($\bar{M}_w$ = 5.8 × 10^4, $\bar{M}_n$ = 3.4 × 10^4). This indicates that GPC underestimates the $\bar{M}_w$ of polymer **4e** due to a difference in the hydrodynamic size of a coil of polystyrene and the poly(ferrocenylsilane) of the same molecular weight if the former polymer is used for column calibration with THF as solvent. A similar difference (26%) in $\bar{M}_w$ was found previously upon analysis of the symmetrically substituted poly(ferrocenylsilane) **2** (R = *n*-Bu) by LALLS and GPC using polystyrene standards in THF.[8a] The second virial coefficient, A_2, found for polymer **4e** was (3.3 ± 0.1) × 10^{-4} mol cm^2 g^{-2}, indicating that solvent/polymer interactions are favorable for this system.

Combustion-based elemental analysis data for polymers **4a–4g** were found to be in good agreement with the assigned structures for hydrogen, but the values obtained for carbon were low by ca. 0.5–4%. Similarly, low carbon analyses were also found for the symmetrically substituted poly(ferrocenylsilanes) **2** (R = Me, Et, *n*-Bu, and *n*-Hex) and this was attributed to the formation of thermally stable, oxidation-resistant ceramics at elevated temperatures.[8a] Indeed, we have shown that poly(ferrocenylsilanes) function as preceramic polymers to yield iron silicon carbide materials on pyrolysis above 500 °C.[8c]

Thermal Transition Behavior and Morphology of Poly(ferrocenylsilanes) 4a–4g. Previous studies of symmetrically substituted poly(ferrocenylsilanes) **2** by differential scanning calorimetry (DSC), dynamic mechanical analysis (DMA), and wide-angle X-ray scattering (WAXS) have shown that **2** (R = *n*-Hex) is amorphous whereas analogous polymers with shorter hydrocarbon side groups, especially **2** (R = *n*-Bu), are capable of showing significant order, particularly when samples of these materials are annealed.[6,7,8a,d,9c] In order to examine the conformational flexibility and morphology of unsymmetrically substituted poly(ferrocenylsilanes), the thermal transition behavior of **4a–4g** was investigated. With the exception of polymers **4a** and **4d**, DSC showed no evidence for melting transitions for the polymer samples studied. Samples of **4a** which had been annealed at 70 °C for 24 h showed two very weak endothermic transitions at 87 and 102 °C, which were not observed on subsequent scans. This is reminiscent of the behavior of annealed samples of **2** (R = *n*-Bu) which show melting transitions at 116 and 129 °C.[6] In the case of polymer **4d**, a large melting endotherm at 16 °C was detected with a corresponding exotherm detected on cooling (Figure 4). In the absence of melting transitions for other poly(ferrocenylsilanes) such as **4b**, **4e**, and **4f** we rationalize this transition for **4d** by the crystallization of the octadecyl side groups below this temperature. The morphology of the unsymmetrical poly(ferrocenylsilanes) **4a–4g** was also investigated by WAXS at 25 °C. The scattering patterns for **4b**, **4c**, **4e**, **4f**, and

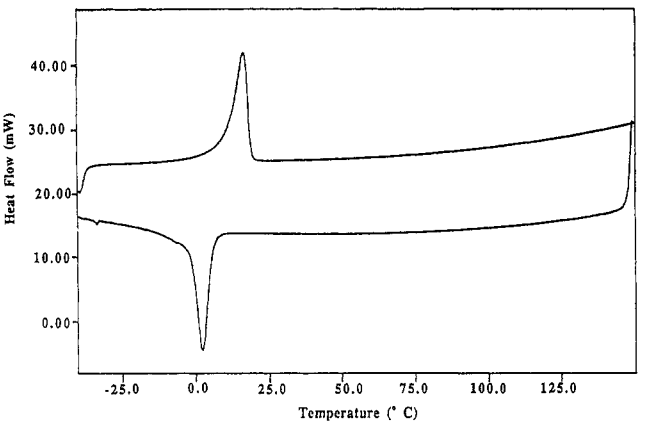

Figure 4. DSC thermogram for poly(ferrocenylsilane) **4d**.

4g were broad and featureless, which confirmed that these polymers were amorphous with no sign of even significant short-range order. In addition, the WAXS pattern for **4d** showed only amorphous halos which was as expected since the T_m detected by DSC at 16 °C was below room temperature. The WAXS pattern of **4a** showed the presence of significant short-range order with a fairly sharp peak corresponding to a *d* spacing of ca. 6.4 Å superimposed on amorphous halos.

The glass transitions determined for **4a–4g** are listed in Table 1. In all cases, T_g's with small changes in heat capacity were detected. Similarly, weak glass transitions were previously detected for the symmetrical poly(ferrocenylsilanes) **2** where the T_g values were found to vary from −26 °C for **2** (R = *n*-Hex) to +33 °C for **2** (R = Me).[8a] In general, the T_g values of **4a–4g** increase with the steric bulk and rigidity of the substituents at silicon. Thus, the presence of side groups such as trifluoropropyl, phenyl, ferrocenyl, or norbornyl was found to increase the T_g value of the poly(ferrocenylsilanes) **4b**, **4e**, **4f**, and **4g** relative to that of the analogous methyl-substituted polymer **2** (R = Me) (T_g = 33 °C). Considering the situation for **4f** it is noteworthy that significant increases in the T_g of organic polymers have previously been detected upon introduction of ferrocenyl groups into the side chain structure.[19] Poly(ferrocenylsilane) **4d**, which exists as a gum at room temperature, was shown by DSC and DMA to possess a weak, yet resolvable glass transition at 1 °C which preceded the melt transition at 16 °C. The flexible *n*-$C_{18}H_{37}$ substituent in **4d** presumably tends to push the polymer chains apart which results in an increase in the free volume, consequently lowering the T_g value relative to that of the other unsymmetrical poly(ferrocenylsilanes). A similar argument was used to explain the lower T_g of **2** (R = *n*-Hex) (−26 °C) relative to that of **2** (R = Me) (T_g = 33 °C).[8a]

Cyclic Voltammetry of the Poly(ferrocenylsilanes) 4a–4g. The symmetrically substituted poly(ferrocenylsilane) **2** (R = Me)[3] and, subsequently, the analogous polymers with longer *n*-alkyl side chains **2** (R = Et, *n*-Bu, and *n*-Hex)[6,7,9c,10] have been shown to exhibit two reversible oxidation waves with shapes that are significantly modified by electrode adsorption effects. The observed electrochemical behavior has been attributed to the presence of interactions between the iron centers which leads to initial oxidation at alternating iron sites followed by the subsequent oxidation at the iron centers in between.[3,7] This explanation has been fully supported by recent cyclic voltammetric studies of well-defined oligo(ferrocenyldimethylsilanes), prepared by anionic ring-opening oligomerization of **1** (R = Me), which exhibit electrochemical behavior which increasingly resembles that of the high molecular weight polymer as the chain length increases.[11]

The cyclic voltammograms of the unsymmetrically substituted poly(ferrocenylsilanes) **4a–4e** and **4g** in CH_2Cl_2 were found to be essentially similar to those previously reported for the symmetrically substituted polymers, and that of **4g** is shown as a representative example in Figure 5. The first wave (at $^1E_{1/2}$) occurs at approximately the same potential as the oxidation of ferrocene, and the second (at $^2E_{1/2}$) occurs at a significantly more positive voltage (Table 2). The peak separation ΔE, which gives a useful measure of the interaction between the transition metal

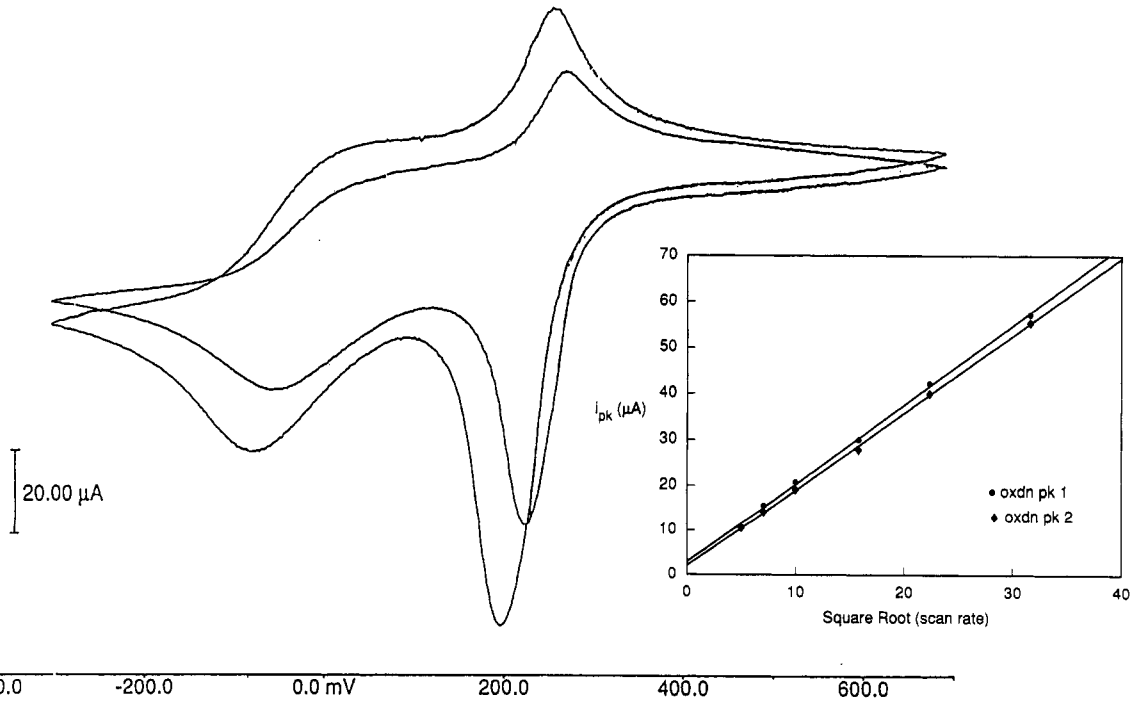

Figure 5. Cyclic voltammograms of a 5 × 10^{-3} M CH_2Cl_2 solution of **4g** obtained at scan rates of 100 and 250 mV/s at 25 °C. The *x*-axis scale is referenced to the ferrocene/ferrocenium ion couple at E = 0.0 mV. Also shown are plots of i_{pk} vs the square root of the scan rate for the two oxidation peaks observed for **4g**.

Table 2. Electrochemical Data for the Unsymmetrical Poly(ferrocenylsilanes) 4a–4g

polymer	R	R′	$^1E_{1/2}$ (V)[a]	$^2E_{1/2}$ (V)[a]	ΔE (V)[b]
4a	Me	H	−0.06	0.12	0.18
4b	Me	$CH_2CH_2CF_3$	0.07	0.23	0.16
4c	Me	$CH{=}CH_2$	0.01	0.21	0.20
4d	Me	n-$C_{18}H_{37}$	−0.02	0.24	0.26
4e	Me	Ph	0.00	0.22	0.22
4f	Me	Fc[d]	−0.03	0.17[c]	0.20
4g	Me	Nor[d]	−0.03	0.23	0.26

[a] $^1E_{1/2}$ and $^2E_{1/2}$ refer to the half-wave potentials for the first and second oxidation waves, respectively, and are relative to the ferrocene/ferrocenium ion couple at 0.00 V which was used as an internal reference. All potentials listed were obtained at scan rates of 250 mV s^{-1}. $E_{1/2} = [E_p(ox) + E_p(red)]/2$. [b] $\Delta E = {}^2E_{1/2} - {}^1E_{1/2}$. [c] A third wave at $^3E_{1/2} = 0.40$ V was detected for this polymer. This corresponds to a value of $\Delta E = 0.23$ V between the second and third waves. [d] Fc = ferrocenyl [(η-C_5H_4)Fe(η-C_5H_5)], Nor = 5-norbornyl.

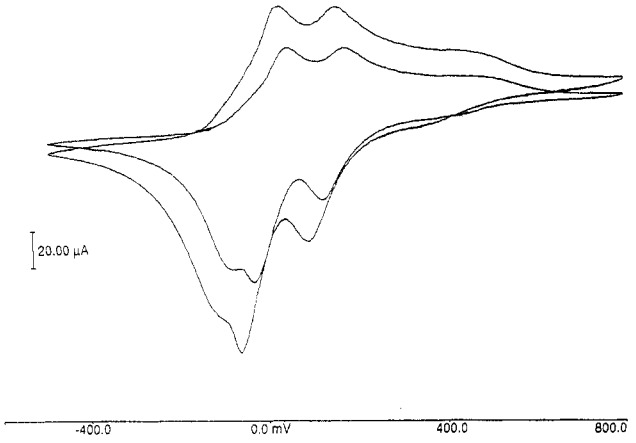

Figure 6. Cyclic voltammograms of a 5×10^{-3} M CH_2Cl_2 solution of **4f** obtained at scan rates of 100 and 250 mV/s at 25 °C. The x-axis is referenced to the ferrocene/ferrocenium ion couple at $E = 0.0$ mV.

centers,[10,20] varies from 0.16 V (for **4b**) to 0.26 V (for **4d** and **4g**), which may be a consequence of substituent-dependent electronic or conformational effects. For polymers **4a–4g**, plots of current vs the square root of the scan rate were linear over the range of scan rates employed (25–1000 mV s^{-1}) for both oxidation waves which indicated that the electron transfer was essentially diffusion controlled. This is illustrated by the insert in Figure 5.

As expected, the cyclic voltammogram of the ferrocenyl-substituted polymer **4f** was found to be more complex than that observed for the others due to the presence of both skeletal and pendent redox centers. The cyclic voltammogram of this material (Figure 6) showed three reversible redox events at $^1E_{1/2} = -0.03$ V, $^2E_{1/2} = 0.17$ V, and $^3E_{1/2} = 0.40$ V vs the ferrocene/ferrocenium ion couple of which the first was the most intense. Such a response is consistent with an initial oxidation at $^1E_{1/2}$ which involves the essentially noninteracting ferrocenyl units in the side chain or, alternatively, nonadjacent ferrocenyl sites in the side chain and in the polymer backbone,[21] followed by sequential oxidation of the iron centers present in the remaining two environments at the higher potentials $^2E_{1/2}$ and $^3E_{1/2}$. The postulated variation of this process involving the initial oxidation at the ferrocenyl side groups is illustrated in Scheme 2. Interestingly, the waves associated with the oxidation at the most highly anodic potential $^3E_{1/2}$ were very broad and this possibly reflects the relatively slow electron transfer kinetics involving iron atoms completely surrounded by positively charged Fe(III) centers.

Summary

A series of unsymmetrical poly(ferrocenylsilanes) **4a–4g** have been prepared from the thermal ROP of the appropriate ring-tilted [1]silaferrocenophane precursors. It is significant to note that even the monomers with relatively bulky side groups such as ferrocenyl and norbornyl polymerize to yield high molecular weight products. Generally, ROP processes are very sensitive to the size of the side group and with sterically demanding substituents they become thermodynamically unfavorable.[22] The successful ROP of **3f** and **3g** is presumably a reflection of the high intrinsic strain present in these molecules which has been measured to be ca. 80 kJ mol^{-1} for **1** (R = Me).[3,6] The poly(ferrocenylsilanes) **4a** and **4d** show evidence of ordered structures, particularly in the case of the latter which possesses a T_m at 16 °C that was attributed to side chain crystallization. These results indicate that detailed and systematic studies of the morphology of poly(ferrocenylsilanes) represent a significant and interesting area for future research. Polymers **4a–4e** and **4g** possess electrochemical properties which are similar to those of symmetrically substituted poly(ferrocenylsilanes) **2** and which are indicative of significant interactions between the iron centers in the polymer backbone. Cyclic voltammetric studies of the poly(ferrocenylsilane) **4f** with pendent ferrocenyl groups suggest that interactions also exist between the skeletal iron atoms and those in the side group structure. Further studies of this interesting class of polymers and related materials are in progress, and the results of these studies will be reported shortly.

Acknowledgment. We thank the Natural Science and Engineering Research Council of Canada (NSERC) and the Institute for Chemical Science and Technology (ICST) for the financial support of this work. We also thank the University of Toronto for an Open Fellowship for Y.N. and D.A.F., the Deutscher Akademischer Austauschdienst (DAAD) for a Postdoctoral Fellowship for R.Z., and the Ontario Center of Materials Research (OCMR) for a scholarship to C.R.J.

Scheme 2

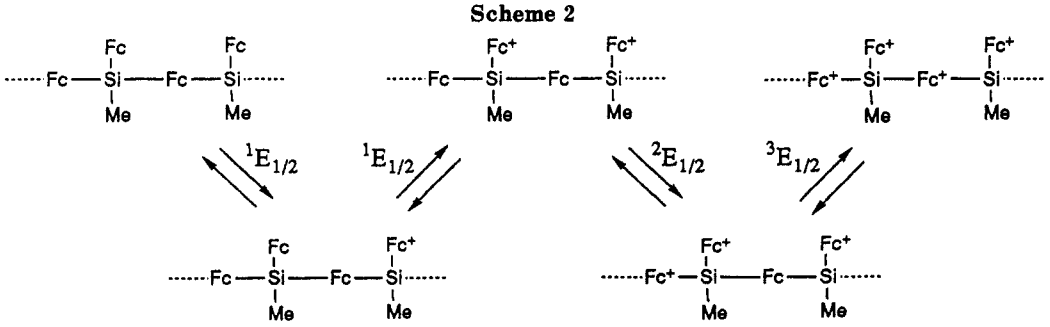

References and Notes

(1) See, for example: (a) Wright, M. E.; Sigman, M. S. *Macromolecules* **1992**, *25*, 6055. (b) Fyfe, H. B.; Mlekuz, M.; Zargarian, D.; Taylor, N. J.; Marder, T. B. *J. Chem. Soc., Chem. Commun.* **1991**, 188. (c) Allcock, H. R.; Dodge, J. A.; Manners, I.; Riding, G. H. *J. Am. Chem. Soc.* **1991**, *113*, 9596. (d) Roesky, H. W.; Lücke, M. *Angew. Chem., Int. Ed. Engl.* **1989**, *28*, 493. (e) Davies, S. J.; Johnson, B. F. G.; Khan, M. S.; Lewis, J. *J. Chem. Soc., Chem. Commun.* **1991**, 187. (f) Tenhaeff, S. C.; Tyler, D. R. *J. Chem. Soc., Chem. Commun.* **1989**, 1459. (g) Neuse, E. W.; Bednarik, L. *Macromolecules* **1979**, *12*, 187. (h) Sturge, K. C.; Hunter, A. D.; McDonald, R.; Santarsiero, B. D. *Organometallics* **1992**, *11*, 3056. (i) Pollagi, T. P.; Stoner, T. C.; Dallinger, R. F.; Gilbert, T. M.; Hopkins, M. D. *J. Am. Chem. Soc.* **1991**, *113*, 703. (j) Bayer, R.; Pohlmann, T.; Nuyken, O. *Makromol. Chem. Rapid Commun.* **1993**, *14*, 359. (k) Gonsalves, K.; Zhanru, L.; Rausch, M. V. *J. Am. Chem. Soc.* **1984**, *106*, 3862. (l) Brandt, P. F.; Rauchfuss, T. B. *J. Am. Chem. Soc.* **1992**, *114*, 1926. (m) Dembek, A. A.; Fagan, P. J.; Marsi, M. *Macromolecules* **1993**, *26*, 2992. (n) Gilbert, A. M.; Katz, T. J.; Geiger, W. E.; Robben, M. P.; Rheingold, A. L. *J. Am. Chem. Soc.* **1993**, *115*, 3199. (o) Nugent, H. M.; Rosenblum, M.; Klemarczyk, P. *J. Am. Chem. Soc.* **1993**, *115*, 3848.

(2) (a) Sheats, J. E.; Carraher, C. E.; Pittman, C. U. *Metal Containing Polymer Systems*; Plenum: New York, 1985. (b) *Inorganic and Organometallic Polymers*; Zeldin, M., Wynne, K., Allcock, H. R., Eds.; ACS Symposium Series 360; Washington, DC, 1988. (c) *Inorganic Polymers*; Mark, J. E., Allcock, H. R., West, R., Eds.; Prentice Hall: New York, 1992. (d) Allcock, H. R. *Adv. Mater.* **1994**, *6*, 106. (e) Manners, I. *Annu. Rep. Prog. Chem., Sect. A: Inorg. Chem.* **1991**, 77. (f) Manners, I. *Ibid.* **1992**, 93.

(3) Foucher, D. A.; Tang, B. Z.; Manners, I. *J. Am. Chem. Soc.* **1992**, *114*, 6246.

(4) (a) Foucher, D. A.; Manners, I. *Makromol. Chem., Rapid Commun.* **1993**, *14*, 63. (b) Ziembinski, R.; Honeyman, C.; Mourad, O.; Foucher, D. A.; Rulkens, R.; Liang, M.; Ni, Y.; Manners, I. *Phosphorus, Sulfur Silicon Relat. Elem.* **1993**, *76*, 219.

(5) (a) Nelson, J. M.; Rengel, H.; Manners, I. *J. Am. Chem. Soc.* **1993**, *115*, 7035. (b) Nelson, J. M.; Lough, A. J.; Manners, I. *Angew. Chem., Int. Ed. Engl.* **1994**, *33*, 989.

(6) Manners, I. *Adv. Mater.* **1994**, *6*, 68.

(7) Manners, I. *J. Inorg. Organomet. Polym.* **1993**, *3*, 185.

(8) (a) Foucher, D. A.; Ziembinski, R.; Tang, B. Z.; Macdonald, P. M.; Massey, J.; Jaeger, R.; Vancso, G. J.; Manners, I. *Macromolecules* **1993**, *26*, 2878. (b) Finckh, W.; Tang, B. Z.; Foucher, D. A.; Zamble, D. B.; Ziembinski, R.; Lough, A.; Manners, I. *Organometallics* **1993**, *12*, 823. (c) Tang, B. Z.; Petersen, R.; Foucher, D. A.; Lough, A.; Coombs, N.; Sodhi, R.; Manners, I. *J. Chem. Soc., Chem. Commun.* **1993**, 523. (d) See: Manners, I. In *Inorganic and Organometallic Polymers*: Allcock, H. R., Wynne, K., Wisian-Neilson, P., Eds.; ACS Symposium Series; Washington, DC (in press).

(9) For the work of other groups on poly(ferrocenylsilanes) see: (a) Rosenberg, H. U.S. Pat. 3,426,053, 1969. (b) Neuse, E. W.; Rosenburg, H. *J. Macromol. Sci. Rev., Macromol. Chem.* **1970**, *C4* (1), 110–111. (c) Nguyen, M. T.; Diaz, A. F.; Dement'ev, V. V.; Pannell, K. H. *Chem. Mater.* **1993**, *5*, 1389.

(10) Foucher, D. A.; Honeyman, C.; Nelson, J. M.; Tang, B. Z.; Manners, I. *Angew. Chem., Int. Ed. Engl.* **1993**, *32*, 1709.

(11) Rulkens, R.; Lough, A. J.; Manners, I. *J. Am. Chem. Soc.* **1994**, *116*, 797.

(12) We have previously briefly reported the synthesis of the unsymmetrically substituted poly(ferrocenylsilanes) **4a–4g** in review articles. See refs 6 and 7.

(13) ROP is known for a variety of organosilicon rings. See, for example: (a) Cypryk, M.; Gupta, Y.; Matyjaszewski, K. *J. Am. Chem. Soc.* **1991**, *113*, 1046. (b) Sargeant, S. J.; Zhou, S. Q.; Manuel, G.; Weber, W. P. *Macromolecules* **1992**, *25*, 2832. (c) West, R.; Hayase, S.; Iwahara, T. *J. Inorg. Organomet. Polym.* **1991**, *1*, 545. (d) Suzuki, M.; Obayashi, T.; Saegusa, T. *J. Chem. Soc., Chem. Commun.* **1993**, 717. (e) Wu, H. J.; Interrante, L. V. *Chem. Mater.* **1989**, *1*, 564. (f) Suzuki, M.; Obayashi, T.; Saegusa, T. *J. Chem. Soc., Chem. Commun.* **1993**, 717.

(14) (a) Bishop, J. J.; Davidson, A.; Katcher, M. L.; Lichtenberg; D. W.; Merrill, R. E.; Smart, J. C. *J. Organomet. Chem.* **1971**, *27*, 241. (b) Fish, R. W.; Rosenblum, M. *J. Org. Chem.* **1965**, *30*, 1253.

(15) Pannell, K.; Rozell, J. M.; Zeigler, J. M. *Macromolecules* **1988**, *21*, 276.

(16) (a) Osborne, A. G.; Whitley, R. H. *J. Organomet. Chem.* **1975**, *101*, C27. (b) Stoeckli-Evans, H.; Osborne, A. G.; Whiteley, R. H. *Helv. Chim. Acta* **1976**, *59*, 2402. (c) Fischer, A. B.; Kinney, J. B.; Staley, R. H.; Wrighton, M. S. *J. Am. Chem. Soc.* **1979**, *101*, 6501. (d) Osborne, A. G.; Whiteley, R. H.; Meads, R. E. *J. Organomet. Chem.* **1980**, *193*, 345.

(17) Heberhold, M.; Brendel, H. D.; Nuyken, O.; Pöhlmann, T. *J. Organomet. Chem.* **1991**, *413*, 65.

(18) Marsmann, H. In *Oxygen-17 and Silicon-29*; Diehl, P., Fluck, E., Kosfeld, R., Eds.; Springer-Verlag: New York, 1981.

(19) Pittman, C. U.; Lai, J. C.; Vandepool, D. P.; Good, M.; Prado, R. *Macromolecules* **1970**, *3*, 746.

(20) Dong, T. Y.; Hwang, M. Y.; Wen, Y.; Hwang, W. S. *J. Organomet. Chem.* **1990**, *391*, 377 and references cited therein.

(21) The first redox process at $^1E_{1/2}$ shows evidence for a shoulder on the reduction wave which suggests that the initial oxidations do not proceed at exactly the same potential. This is indicative of a very small but nonnegligable degree of interaction between the ferrocenyl centers involved. The presence of only very small interactions between ferrocenyl side groups is consistent with the observation of a single reversible oxidation wave for poly(vinylferrocene). See: Brown, G. M.; Meyer, T. J.; Cowan, D. O.; Levanda, C.; Kaufman, F.; Roling, P. V.; Rausch, M. D. *Inorg. Chem.* **1975**, *14*, 506.

(22) For an elegant illustration of the effects of steric bulk on the polymerization behavior of cyclic silanes see ref 13a.